Fractal Dimension and Roughness of Profiles and Surfaces*

J. G. Moreira[1], *J. Kamphorst Leal da Silva*[1] *and S. Oliffson Kamphorst*[2]

[1] Departamento de Física, Instituto de Ciências Exatas,
Universidade Federal de Minas Gerais,
C.P. 702, 30161-970 Belo Horizonte, Brazil

[2] Departamento de Matemática, Instituto de Ciências Exatas,
Universidade Federal de Minas Gerais,
C.P. 702, 30161-970 Belo Horizonte, Brazil

1 Introduction

The complex forms of nature are too irregular to fit into a traditional geometrical setting. On the other hand, they are nicely described in terms of the concepts of fractal geometry [1]. These forms often present statistical scale invariance and can be characterized by few parameters like fractal dimensions and scaling exponents. A self-similar fractal is invariant under an isotropic length scale transformation – all the different directions scale in the same way. We can cite as examples coastlines [1], percolation clusters [1, 2], colloidal aggregates [3] etc. When an object is invariant under a transformation with different length scales in different directions it is a self-affine fractal [4]. Recent works have demonstrated that a wide class of processes lead to objects with self-affine properties: plots of random walks [1, 2], interfaces in far-from-equilibrium systems [5] and interfaces resulting from growth processes [5, 6, 7].

In many circumstances the interface $f(\mathbf{x})$ generated from a smooth surface by some stochastic process becomes rough. These interfaces can be characterized by its roughness $W(f, L)$. It is defined as the fluctuation around the average of the height f at scale L, namely

$$W^2(f, L) = \langle f^2(\mathbf{x}) \rangle_L - \langle f(\mathbf{x}) \rangle_L^2 \ . \tag{1}$$

where $\langle ... \rangle_L$ means average over x in the scale L. For self-affine interfaces, the roughness $W(f, L)$ scales with the linear size L of the surface by an exponent H ($W \sim L^H$), called the roughness or Hurst exponent. This exponent has been received a lot of attention in the last years and has been used to characterize different phenomena in many distinct subjects as for example, biology [8] and fractures [9].

In this work we consider the connection between generalized roughness and fractal dimension for interfaces in dimension $d = 2$ (profiles) and $d = 3$ (surfaces).

* This research was supported in part by Conselho Nacional de Desenvolvimento Científico e Tecnológico (CNPq) and in part by Fundação de Amparo à Pesquisa do Estado de Minas Gerais (Fapemig), Brazilian agencies.

The profiles and surfaces $f(\mathbf{x})$ are characterized by a fractal dimension D and by a roughness or Hurst exponent H. By fractal dimension we mean the Minkowski-Bouligand dimension, box dimension [1] or other equivalent one. Essentially the fractal dimension is related to the scaling properties of d-dimensional volumes of a cover for the interface and the Hurst exponent measures the scaling of the average of a local roughness $w(\mathbf{x}, \epsilon)$, evaluated in a $\epsilon-$neighborhood of $\mathbf{x}$. The rate of convergence to zero of $W(f, \epsilon) = \int w(\mathbf{x}, \epsilon)\, d\mathbf{x}$ as ϵ goes to zero defines the roughness exponent H. We show that H is related to the fractal dimension D through $H = d - D$.

We propose a new numerical algorithm for the evaluation of D, based on a roughness around the local linear fit. This method is tested on self-affine curves with known fractal dimensions: the Weierstrass function and the fractional Brownian motion. The estimates of D are then compared with the ones obtained from methods of the literature.

This work is organized as follows. In the next section we present the mathematical aspects of the connection between the generalized roughness and the Minkowski-Bouligand dimension. Both the cases of profiles and surfaces are considered. The Weierstrass function and the fractional Brownian motion are briefly presented in section 3. In section 4 we define the new numerical algorithm based on the generalized roughness for the evaluation of D. The results obtained for the two standard profiles of section 3 are also discussed in this section. A summary of ours results is presented in the last section.

2 Generalized Roughness and Fractal Dimension

In this section, we present a proof of the relation $D = d - H$ for arbitrary graphs of functions of one (profiles, $d = 2$) or two (surfaces, $d = 3$) real variables. Although this relation was for long known for exact self-affine fractals [10], and can also be derived from scaling arguments for statistical self-affine profiles as the fractional Brownian motion [2, 11], there is no rigorous proof, at least at our knowledge, that it works in the general case. We should point out that for the general case of statistical fractals, even the notion of fractal dimension can be viewed as a first approximation to the microscopic structure, and a multifractal analysis [2, 5, 6, 12] is necessary. Our proof relays in the fact the fractal dimension as well as the roughness exponent, measures how far a fractal interface is from any smooth function that one use to approximate it.

Throughout this work the term interface refers to the graph G_f of a function f of a real variable x, or two real variables x, y, continuous on its domain of definition. To uniformize notation we call the variable $\mathbf{x}$, meaning x or (x, y) depending on the dimension d we are, so the interface is the graph of $f(\mathbf{x})$. Without loss of generality, we fix the domain of definition of f as the interval $[0, 1]$ or the square $[0, 1] \times [0, 1]$ and call this domain $\mathcal{D}$. We are interested in the evaluation of the fractal dimension of the graph G_f. We shall investigate the Minkowski-Bouligand dimension [13], which is equivalent to the box dimension[10]. Although these definitions of dimension characterize the local fractal properties of profiles, they can differ from the Hausdorff dimension [2, 4, 6, 14]. In this work we do not evaluate the Hausdorff dimension. Upper bounds for the Hausdorff dimension of graphs of functions, as well as a very nice discussion about fractal dimensions, can be found in Falconer [14].

Tricot et al.[15] have used the concept of generalized covers in order to demonstrate the equivalence of box and Minkowski-Bouligand dimension. They have shown that for covers by suitable geometric figures (satisfying some non-distortion relations) the fractal dimension is given by

$$D = \lim_{\epsilon \to 0} \left[d - \frac{\ln |U(\epsilon)|_d}{\ln \epsilon} \right] \quad , \tag{2}$$

where $|U(\epsilon)|_d$ is the d-dimensional volume of the union of figures $U(\epsilon)$ covering the graph G_f. Equation (2) gives the same dimension for all generalized covers. For example, the figures are balls of radius ϵ centered on $(\mathbf{x}, f(\mathbf{x}))$ in the Minkowski-Bouligand cover and d-dimensional cubes in the box-dimension evaluation. The numerical algorithms for $d = 2$ resulting from the Minkowski-Bouligand and box dimensions have been analized in Dubuc et al. [16]. The estimates obtained for D were poor when these algorithms have been applied in profiles with known dimensions. It has been found that the basic problem was the "thickness" of the covers. In order to develop better numerical algorithms, Dubuc et al.[16] have introduced two alternating ways of evaluation of fractal dimension: the *horizontal structuring element method* and the *variation method*. Both of them are based on the idea of building covers with intervals instead of geometrical figures. The first uses horizontal segments and the second vertical ones. The idea was extended to n dimensional graphs by Dubuc & Tricot [17].

For further use, let us present briefly the variation method for $d = 2$ [15, 16] and $d = 3$ [18]. Since we are interested in fractal graphs, we can assume that f is nowhere or almost nowhere differentiable. The fractal dimension of the graph is related to the $\epsilon-$oscillation $v(\mathbf{x}, \epsilon)$ of the function f. The $\epsilon-$variation of f in the region $\mathcal{D}$ is defined by

$$V(\epsilon, f) = \int_{\mathcal{D}} v(\mathbf{x}, \epsilon) \, d\mathbf{x} \quad , \tag{3}$$

$$v(\mathbf{x}, \epsilon) = \sup_{\mathbf{x}' \in R_\epsilon(\mathbf{x})} f(\mathbf{x}') - \inf_{\mathbf{x}' \in R_\epsilon(\mathbf{x})} f(\mathbf{x}') \quad . \tag{4}$$

Here $R_\epsilon(\mathbf{x})$ is a rectangle of side ϵ centered at $\mathbf{x}$ or its intersection with $\mathcal{D}$ and is called an $\epsilon-$ neighborhood of $\mathbf{x}$. The $\epsilon-$oscillation is also equivalent to the *maximum range* of f in $R_\epsilon(\mathbf{x})$ as defined in [14]. For $d = 2$, the union of vertical segments $S(x, \epsilon) = \{x\} \times [\inf_{x' \in R_\epsilon(x)} f(x'), \sup_{x' \in R_\epsilon(x)} f(x')]$ is a cover for G_f and has, by definition, area equal to the ϵ-variation of f, $|\mathcal{U}(\epsilon)|_2 = V(\epsilon, f)$. It can be shown [15, 17] that $V(\epsilon, f)$ leads to the fractal dimension in any dimension. As long as f is not a constant, we have

$$D = \lim_{\epsilon \to 0} \left[d - \frac{\ln V(\epsilon, f)}{\ln \epsilon} \right] \quad . \tag{5}$$

Intuitively this defines the fractal dimension as the scaling exponent of the area or volume occupied by the graph G_f. Essentially, $V(\epsilon, f)$ measures the difference between the area (volume) under the upper approximation of f at scale ϵ and the lower approximation of f at the same scale.

The idea we introduce now, is to define a finer cover in $d = 2$ by measuring a local oscillation of the function f by a local roughness, defined by

$$w^2(x, \epsilon) = \frac{1}{2\epsilon} \int_{x-\epsilon}^{x+\epsilon} \left[f(x') - \langle f(x')\rangle_\epsilon\right]^2 \, dx' \ , \tag{6}$$

$$\langle f(x)\rangle_\epsilon = \frac{1}{2\epsilon} \int_{x-\epsilon}^{x+\epsilon} f(x') \, dx' \ . \tag{7}$$

Note that $\langle f(x)\rangle_\epsilon$ is a local average of the function f. Actually this local average function may be replaced by any smooth interpolating function. It can be replaced by, for example, the local RMS straight line in order to have a better local fit. A sufficient condition is that

$$0 < w(x, \epsilon) \leq v(x, \epsilon) \quad \text{for all } x \text{ and all } \epsilon > 0 \ . \tag{8}$$

We can see that $w(x, \epsilon) > 0$ holds for any smooth fitting if we assume that the function f is *nowhere differentiable*. The condition $w(x, \epsilon) \leq v(x, \epsilon)$ means that this cover is finer than the one due to the ϵ oscillation and therefore fits the graph G_f better. For the average of the function $\langle f(x)\rangle_\epsilon$ the condition (8) is easily verified from equations (4) and (6). Now we demonstrate that for oscillations $w(x, \epsilon)$ satisfying (8) we have

$$\lim_{\epsilon \to 0} \frac{\ln W(f, \epsilon)}{\ln \epsilon} = \lim_{\epsilon \to 0} \frac{\ln V(f, \epsilon)}{\ln \epsilon} \ , \tag{9}$$

where we have defined the average roughness $W(f, \epsilon) = \int_0^1 w(x, \epsilon) \, dx$. For every fixed $\epsilon > 0$, $w(x, \epsilon)$ is a continuous strictly positive function of x on the interval $[0, 1]$. Therefore we can find a δ_ϵ such that $w(x, \epsilon) \geq \delta_\epsilon > 0$ for all x. On the other hand, $v(x, \epsilon)$ is also continuous with regard to ϵ and x on compact sets of the plane. Then we can choose ϵ' such that $v(x, \epsilon') \leq \delta_\epsilon$ for all x. Therefore we have

$$V(f, \epsilon') \leq W(f, \epsilon) \leq V(f, \epsilon) \ . \tag{10}$$

Taking the logarithm, dividing by $\ln \epsilon$, considering the limit as ϵ', $\epsilon \to 0$ and using equation (5) we obtain that the fractal dimension D is given by

$$D = 2 - \lim_{\epsilon \to 0} \frac{\ln W(f, \epsilon)}{\ln \epsilon} \ . \tag{11}$$

For self-affine curves we have that $W(f, \epsilon) \sim \epsilon^H$, where H is the Hurst exponent, implying that $D = 2 - H$.

In higher dimension, the proof is compleatly equivalent, we only need to replace x by $\mathbf{x}$, and integrals over $[0, 1]$ by integrals over $\mathcal{D}$, all the compactness arguments still work. Therefore we have

$$D = d - \lim_{\epsilon \to 0} \frac{\ln W(f, \epsilon)}{\ln \epsilon} \ . \tag{12}$$

This equation establishes a formal connection between roughness and fractal dimension in all dimensions. For self-affine interfaces we have a relation between the fractal dimension and the roughness exponent, namely $D = d - H$.

3 Two Standard Self-Affine Profiles

For further use, let us introduce briefly two standard self-affine profiles. The first one is the real cosine Weierstrass function (WF) $f_H(x)$, defined as

$$f_H(x) = \sum_{n=-\infty}^{\infty} b^{-nH} \left[1 - \cos(b^n x)\right] \quad , \tag{13}$$

where $b > 1$ and $0 < H < 1$. Note that the WF has a scaling behavior with different scaling ratios, since $f_H(bx) = b^H f(x)$.

The second one is the trace $B_H(t)$ of the fractional Brownian motion (FBM). $B_H(t)$ is a single-valued function of one real variable (t) and its increments $\Delta B_H(\Delta T) = B_H(t_2) - B_H(t_1)$ have a Gaussian distribution. The variance of this distribution is given by

$$\langle \Delta B_H^2(\Delta t) \rangle \sim \Delta t^{2H} \quad , \tag{14}$$

with $0 < H < 1$, $\Delta t = |t_2 - t_1|$ and $\langle \ldots \rangle$ denotes the ensemble average. There are several algorithms to generate the FBM. We use an algorithm described in Feder [2], page 174,equation (9.25). In Fig. 1 it is shown some typical traces. The FBM is a statistical self-affine object because its scaling properties. If Δt is changed by the factor r, the increments ΔB must be changed by a different factor r^H, since

$$\langle \Delta B_H^2(r\Delta t) \rangle \sim r^{2H} \langle \Delta B_H^2(\Delta t) \rangle \quad . \tag{15}$$

The values of the fractal dimension depends on the way one measures it [2]. In order to obtain the local box dimension we can use a scaling argument. We must cover the trace of the FBM and the graph of WF with small boxes. Then it is easy to obtain that $D = 2 - H$ for both the profiles. A detailed evaluation of D for the WF and FBM can be found in textbooks [2, 6]. We must also observe that a multivariate WF in the continuum limit is equivalent to the multivariate FBM [19].

4 Numerical Algorithm for the Evaluation of D

It is straightforward to develop numerical algorithms to evaluate the dimension D or the roughness exponent by using (11). We will describe the method for $d = 2$ but its extension for $d = 3$ is simple. Suppose that we have $N + 1$ points $f(\frac{n}{N})$ $(n = 0, 1, 2 \ldots N)$ of the digitized profile. In this method, called the roughness around the RMS straight line (SLR), we consider a ϵ neighborhood of each point $x = n/N$ of the digitized profile. First we evaluate the best straight

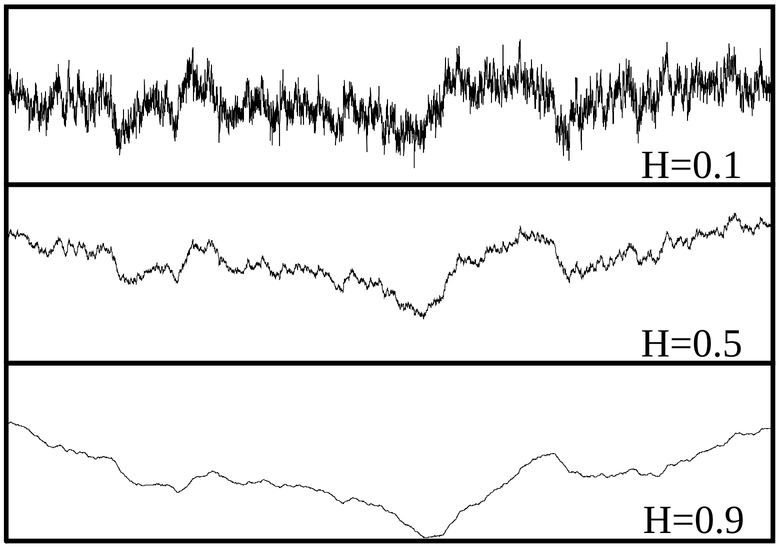

Fig. 1. The fractional Brownian motion trace with $n = 8$ and $M = 700$ for (a) $H = 0.9$; (b) $H = 0.5$; and (c) $H = 0.1$.

line $a_x(n/N) + b_x$ in this interval, with the coefficients a_x and b_x evaluated by the root mean square method. The local roughness is then given by

$$w^2(x,\epsilon) = \frac{1}{\epsilon} \sum_{n \in \epsilon} \left[f(n/N) - \left(a_x \frac{n}{N} + b_x \right) \right]^2 \quad . \tag{16}$$

Observe that this is equivalent to (6). Finally, we obtain the ϵ dependent roughness as

$$W(f,\epsilon) = \frac{1}{N+1} \sum_{x=0}^{1} w(x,\epsilon) \quad . \tag{17}$$

This procedure is repeated for several scales ϵ and the fractal dimension D is given by the slope of the $\ln[\frac{W(f,\epsilon)}{\epsilon^2}] \times \ln(1/\epsilon)$ plot. Due to discreteness, the log-log plot does not give an accurate estimate of D for all scales ϵ. We have defined a smallest scale ϵ_0 and consider all scales of the form $\epsilon_k = c^k \epsilon_0$ $(\epsilon_k < N)$, where $c > 1$ is a constant. Then we evaluate the local slope D_i of the graph by taking a fixed number of successive points starting at k_i. When D_i is almost constant we have a reliable estimate of D. We consider the most frequent value of D_i as the best estimate for the fractal dimension. The error bar is estimated by considering the values near D_i that are significantly frequent.

In order to test the robustness and the efficiency of this algorithm, we evaluate the D dimension of mathematical objects with well known fractal dimension. The first object is the Weierstrass function (WF), defined in (13). The second object is the trace $B_H(t)$ of the fractional Brownian motion (FBM), already presented in the preceding section. The numerical values of D for the WF are shown in Table 1 . The exact fractal dimension is given in first column; the estimates D_{VAR} obtained by using the variation method [16] are shown in the second column; the third column shows the results obtained by the traditional roughness, i. e., the roughness around the mean height (D_{MHR}); the fourth column shows the evaluation of the fractal dimensions obtained by our method (D_{SLR}). The error of the last digit is shown between parentheses.

Table 1. Fractal dimensions D of profiles generated by the Weierstrass function with $b = 2.1$ in the interval $[0.60, 0.61]$; the studied profiles have been digitized with 20000 points; D is the exact value and D_{VAR} is the estimate of the variation method; D_{MHR} and D_{SLR} are the results obtained from the roughness around the local average height and around the local RMS straight line respectively. The error in the last digit is indicated between parenthesis.

D	D_{VAR}	D_{MHR}	D_{SLR}
1.9	1.83(1)	1.898(1)	1.901(1)
1.7	1.655(5)	1.702(2)	1.709(1)
1.5	1.475(1)	1.500(6)	1.515(1)
1.3	1.281(1)	1.292(6)	1.319(1)
1.1	1.096(1)	1.101(3)	1.121(1)

The results for the fractional Brownian motion are shown in Table 2, which is similar to the preceding table. Note that the estimates of the fractal dimension are worst than the ones obtained for the WF.

The $\ln[W(f,\epsilon)/\epsilon^2] \times \ln[1/\epsilon]$ plots of the FBM for three values of H are depicted in Fig. 2. Similar plots have obtained for the WF.

From these plots we evaluate the slope D_i of several intervals of scales ϵ. The $D_i \times i$ plots for the WF and the FBM are shown in Fig. 3 and in Fig. 4, respectively.

Let us discuss now the results obtained for the WF. We have very good

Table 2. Fractal dimensions D of profiles generated by the fractional Brownian motion with $n = 8$ and $M = 700$; the studied profiles have 20000 points; D, D_{VAR}, D_{MHR} and D_{SLR} are defined as in the preceding table.

D	D_{VAR}	D_{MHR}	D_{SLR}
1.9	1.80(2)	1.88(1)	1.87(1)
1.7	1.68(2)	1.725(5)	1.715(5)
1.5	1.52(2)	1.535(5)	1.525(5)
1.3	1.34(2)	1.36(2)	1.320(5)
1.1	1.22(4)	1.24(4)	1.105(5)

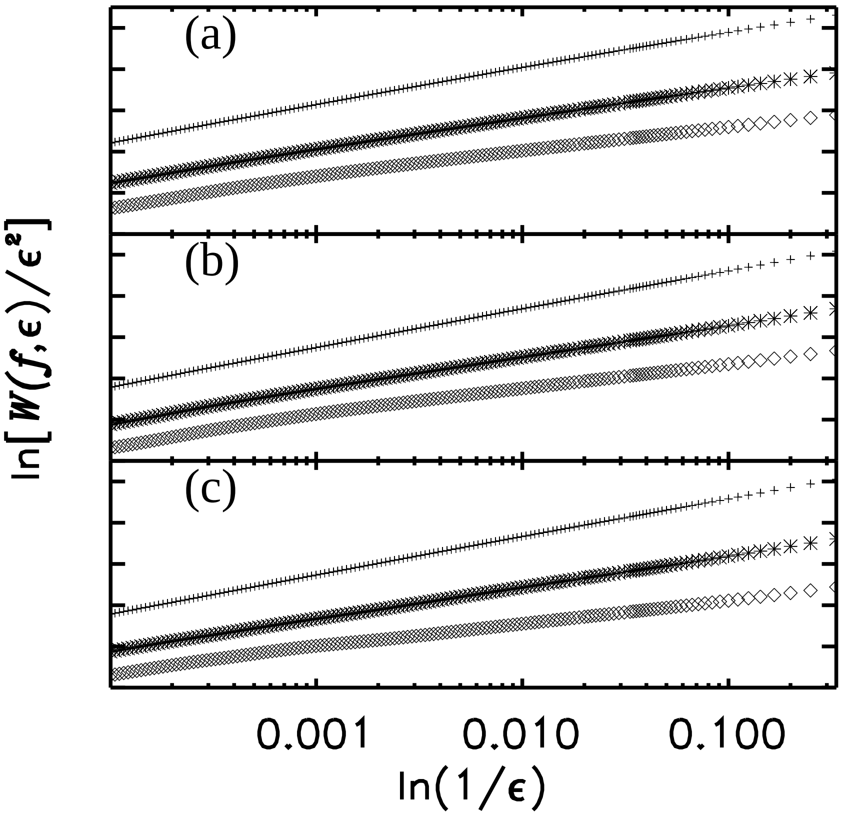

Fig. 2. The $\ln[W(f,\epsilon)/\epsilon^2] \times \ln(1/\epsilon)$ plot of the fractional Brownian motion obtained by (a) the variation method, (b) the MHR method and (c) the SLR method for $H = 0.1$ (+), $H = 0.5$ ($*$) and $H = 0.9$ ($\diamond$).

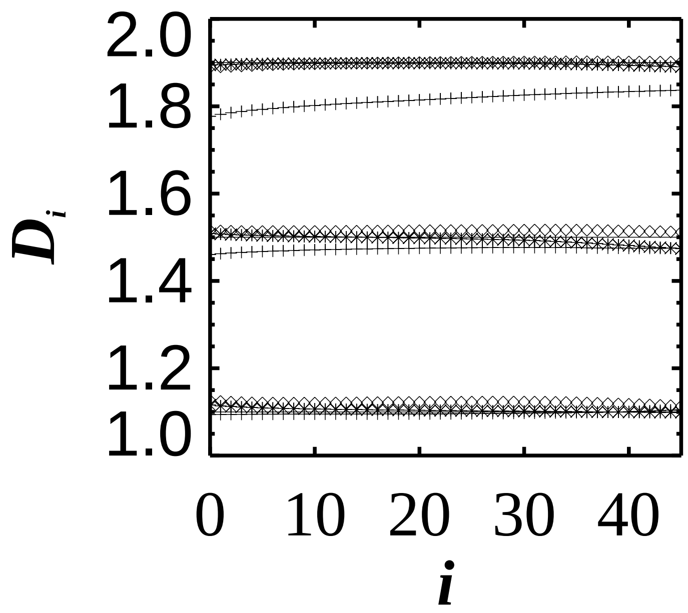

Fig. 3. The graphs of the fractal dimension $D_i \times i$ of the Weierstrass function for three different values of the parameter H. The exact values are represented by solid lines. Shown also are the estimates obtained by the variation $(+)$, the MHR $(*)$ and the SLR $(\diamond)$ methods.

straight lines for the three methods in $\ln[W(f,\epsilon)/\epsilon^2] \times \ln[1/\epsilon]$ plots. In fact, the fitting is much more better than the ones for the FBM. We must observe, however, that exist some differences between the three methods. The results of the variation method at low H (high roughness) only stabilizes for large scales in a value below the expected one. For the other two methods the results are almost stable for all scales and in good agreement with the theoretical value of D. When the roughness is small $(H \sim 0.9)$, the variation method is more stable and the three methods give good results for the fractal dimension.

The results obtained by the three methods for the FBM are not so good as the ones obtained for the WF. For high roughness, the MHR and SLR methods give us a better estimation of D than the variation one. In the cases that the roughness is small, all the methods are not stable for large scales, mainly for the VAR and MHR methods. For this cases, the straight line roughness method is the only one that gives a reliable estimate of the fractal dimension.

The above results can be explained as follows. Figure 5 shows the coverings of the trace of the FBM with an intermediate value of the parameter H. The scales of the plots are the same for the three methods. We can see that the covering of SLR method is the finest and the one of the variation method is very crude.

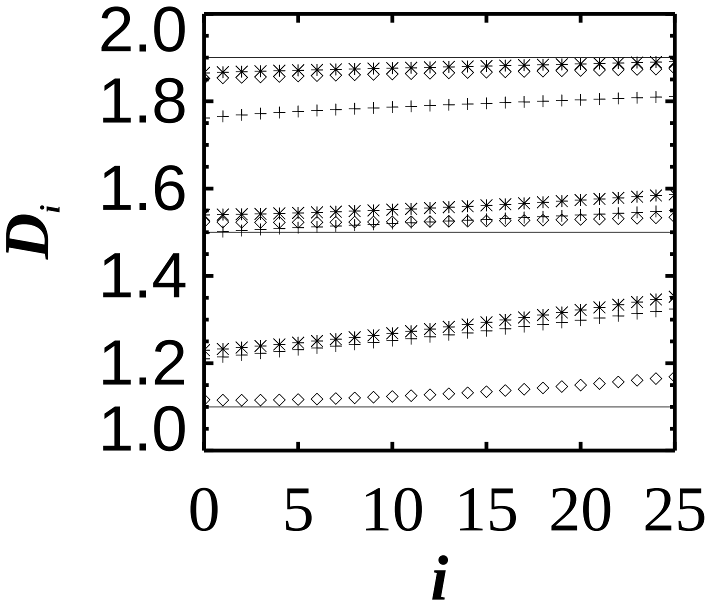

Fig. 4. Figure similar to Fig. 3 for the fractional Brownian motion.

Independent of the test function, the VAR method does not give a good estimate of D for low H because the curve is so rough (see Fig. 1c) implying that the cover is particularly crude. For the WF with $H \sim 0.9$ the profile is quite smooth and the three methods work well. On the other hand, for the FBM trace in the same range of H, the profile is also quite smooth but has some valleys and hills (see Fig. 1a). It means that we have a roughness of large scales, which are not taken in account by the VAR and MHR methods.

All results shown here were obtained for a particular set of parameters described in the captions of the tables. However, we have checked the robustness of the methods by considering the WF and the FBM with other sets of parameters and found similar results. The estimates of D were obtained by visiting each point of the 20,000 ones of the digitized profile. Moreover, the results do not change when the profiles are digitized with less points. For instance, we have studied profiles with 5,000 and 2,000 points and observed a difference only in the last significative digit in the case of 2,000 points.

5 Summary

In conclusion, we have shown that the roughness is closely related to the fractal dimension (Minkowski-Bouligand or box dimensions) of profiles ($d = 2$) and

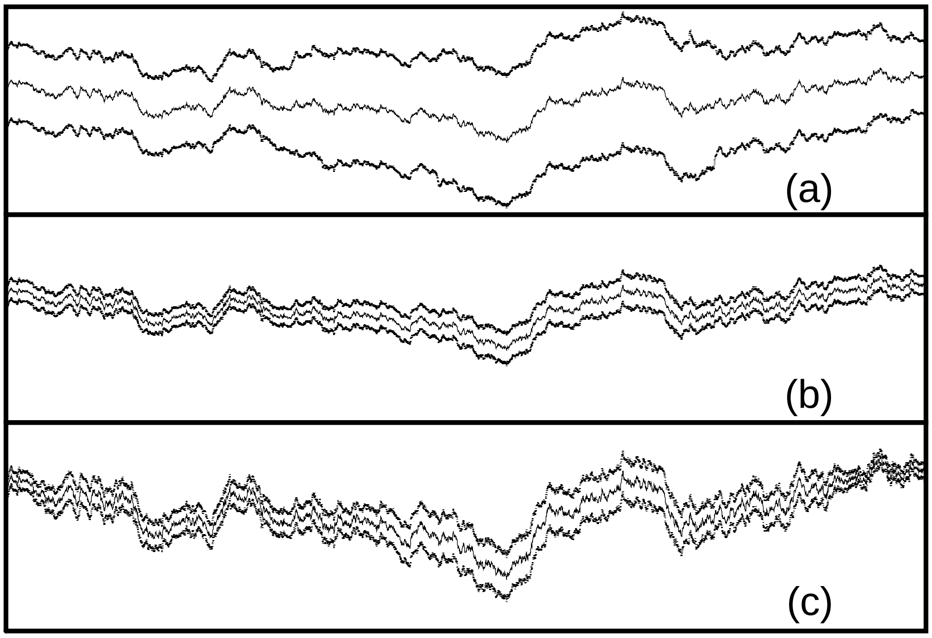

Fig. 5. Covering of the FBM trace with $H = 0.5$ by the (a) VAR; (b) MHR; and (c) SLR methods. The middle curves represent the traces, the top (bottom) curves are obtained by adding (subtracting) the local roughness $w(x, \epsilon)$ to the coordinates of the traces. For the VAR method the roughness is given by Eq. (4). The traces are digitalized with 5,000 points and $\epsilon = 1,000$.

surfaces ($d = 3$) nowhere differentiable. In particular, we have demonstrated a relation between the fractal dimension and the roughness exponent of self-affine fractals, namely $D = d - H$. This has allowed us to present a new numerical algorithm for the evaluation of the fractal dimension or the roughness exponent. This algorithm, based on generalized roughness, is more robust and reliable than the standard ones. We should pointed out that this algorithms is especially useful if one wants to observe the roughness over profiles or surfaces which have an arbitrary shape. This kind of shape is found, for example, in fractures. Finally, let us observe that the numerical algorithms for surfaces ($d = 3$) are equal to the ones for profiles ($d = 2$), except that we must now evaluate the roughness around the best plane in a ϵ neighborhood.

Acknowledgments. The authors wish to thank P. Mendes and A. T. Bernardes for useful discussions.

References

1. B. B. Mandelbrot : "The Fractal Geometry of Nature" (Freeman, San Francisco, 1982).
2. J. Feder, "Fractals" (Plenum, New York, 1988).
3. P. Meakin, J. of Coll. and Inter. Science **134**, 235 (1990).
4. B. B. Mandelbrot in "Fractals in Physics", edited by L. Pietronero and E. Tosatti (North-Holland, Amsterdam 1986), p. 3.
5. "Random Fluctuations and Pattern Growth", edited by H. E. Stanley and N. Ostrowsky (Kluwer, Dordrecht 1988).
6. T. Vicsek, "Fractal Growth Phenomena" (World Scientific, Singapore, 1989).
7. F. Family, Physica A **168**, 561 (1990).
8. H. E. Stanley, S. V. Buldyrev, A. L. Goldberger, Z. D. Goldberger, S. Havlin, R. N. Mantegna, S. M. Ossadnik, C.-K. Peng and M. Simons, Physica A **205** 214 (1994).
9. K. J. Måløy, A. Hansen, E. L. Hinrichsen and S. Roux, Phys. Rev. Lett. **68** 213 (1992).
10. B. B. Mandelbrot, Phys. Scr. **32**, 257 (1985).
11. R. F. Voss, Physica D **38**, 362 (1989).
12. "Dynamics of Fractal Surfaces", edited by F. Family and T. Vicsek (World Scientific, Singapore 1991).
13. G. Bouligand, Bull. Sci. Math. **2**, 185 (1929).
14. K. Falconer, "Fractal Geometry" (John Wiley & Sons, Chichester, 1990).
15. C. Tricot, J. F. Quiniou, D. Wehbi, C. Roques-Carmes and B. Dubuc, Rev. Phys. Appl. **23**, 111 (1988).
16. B. Dubuc, J. F. Quiniou, C. Roques-Carmes, C. Tricot and S. W. Zucker, Phys. Rev. A **39**, 1500 (1989).
17. B. Dubuc and C. Tricot, C. R. Acad. Sci., Paris **306**, 531 (1988).
18. B. Dubuc, S. W. Zucker, C. Tricot, J. F. Quinou and D. Wehbi, Proc. R. Soc. Lond. A **425**, 113 (1989).
19. M. Ausloos and D. H. Berman, Proc. R. Soc. Lond. A **400**, 331 (1985).

This article was processed using the LaTeX macro package with LMAMULT style